Monte Carlo Based Diffusion Coefficients for LMFBR Analysis

Joint International Conference on Supercomputing in Nuclear Applications and Monte Carlo 2010 (SNA + MC2010)
Hitotsubashi Memorial Hall, Tokyo, Japan, October 17 - 21, 2010

Monte Carlo Based Diffusion Coefficients for LMFBR Analysis

Willem F.G. VAN ROOIJEN[1*], Taira HAZAMA[2] and Toshikazu TAKEDA[1]

[1] *Research Institute of Nuclear Energy, University of Fukui, Bunkyo 3-9-1, Fukui-shi, Fukui-ken, 910-8507, Japan*
[2] *Japan Atomic Energy Agency, 1 Shiraki, Tsuruga-shi, Fukui-ken, 919-1279, Japan*

A method based on Monte Carlo calculations is developed to estimate the diffusion coefficient of unit cells. The method uses a geometrical model similar to that used in lattice theory, but does not use the assumption of a separable fundamental mode used in lattice theory. The method uses standard Monte Carlo flux and current tallies, and the continuous energy Monte Carlo code MVP was used without modifications. Four models are presented to derive the diffusion coefficient from tally results of flux and partial currents. In this paper the method is applied to the calculation of a plate cell of the fast-spectrum critical facility ZEBRA. Conventional calculations of the diffusion coefficient diverge in the presence of planar voids in the lattice, but our Monte Carlo method can treat this situation without any problem. The Monte Carlo method was used to investigate the influence of geometrical modeling as well as the directional dependence of the diffusion coefficient. The method can be used to estimate the diffusion coefficient of complicated unit cells, the limitation being the capabilities of the Monte Carlo code. The method will be used in the future to confirm results for the diffusion coefficient obtained with deterministic codes.
KEYWORDS: Diffusion Coefficient, Benoist-formalism, Plate Cell, Critical Experiment, Directional Diffusion Coefficient, Sodium Void Effect

I. Introduction

In cell calculations the diffusion coefficient is commonly calculated using the so-called Benoist-formalism[1)]. In this formalism, several approximations are used to derive at an expression which yields the so-called directional diffusion coefficient $D_k, k = x, y, z$, as a function of the so-called directional collision probability $P_{ij,k}$. This approach has been used in cell calculation codes, e.g. ECCO[2)] and SLAROM-UF[3)]. However, the Benoist-style diffusion coefficient becomes infinite if there are planar voids in the lattice. A planar void is a void region of such a geometry that a slab with infinite lateral dimensions and finite thickness can be fully contained in it[4)]. Planar voids occur naturally in one-dimensional slab cells, but also in rectangular and hexagonal lattices of pins, as illustrated in **Fig. 1**.

Investigations are presently going on to improve the calculation accuracy of the diffusion coefficient of voided unit cells. The main focus is on lattice theory (also known as the fundamental mode approximation) for which the Method of Characteristics has been selected. To provide confirmation of newly developed models, a Monte Carlo based method to calculate the diffusion coefficient of non-voided and voided unit cells has been developed. The method is presented in this paper and results for slab cells are reported. Results of the MOC-based method applied to hexagonal LMFBR cells are reported elsewhere[5)].

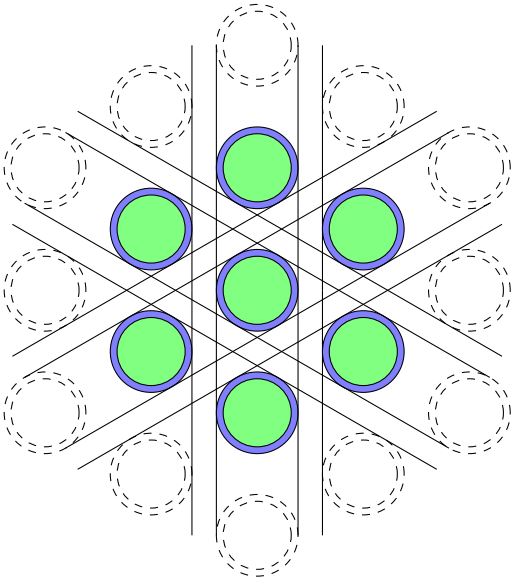

Fig. 1 Planar voids in an infinite lattice of pin cells. The planar void occurs if $P/D > 2/\sqrt{3} \approx 1.15$, which is the case in many fast reactors (P/D: pitch-to-diameter ratio).

II. Theory

Monte Carlo calculations can be used to estimate the diffusion coefficient of a unit cell, for which there appear to be three main approaches:

- One approach is rooted in lattice theory and uses Monte Carlo methods to calculate the average distance between the points of birth and absorption of a neutron[6)].
- The second method is based on the calculation of the mean square path lengths between neutron collisions and derives a diffusion coefficient from the migration area and diffusion length[7)].
- In our work, we follow the work by Milgram[8)], and use standard Monte Carlo techniques to calculate the diffusion coefficient with a method that is completely separate from lattice theory.

The fundamental assumption of diffusion theory is that the diffusion coefficient is the constant of proportionality between the net current at a point and the gradient of the scalar flux at that point[8)]. By making an adequate geometrical model and

*Corresponding author, E-mail: rooijen@u-fukui.ac.jp

tallying the necessary quantities, one can use the fundamental definition of D directly to obtain a cell averaged diffusion coefficient.

1. Unit cell geometry

Unit cells are assumed to be *three-dimensional* and *symmetric*. A lattice is made by an infinite repetition of the unit cells. Unit cells are not required to have any special shape, as long as they can fill up the entire space. The flux is symmetric and periodic with the lattice, while the net current is zero on the boundaries of the cell. In classic lattice theory, the finite size of the system is introduced through a buckling vector. Mathematically, the system is then described as a slab with its boundaries perpendicular to the direction of the buckling. In Monte Carlo calculations, one can simulate this situation by using a collection of unit cells, infinite in two directions and finite in the third direction. It is convenient to choose the finite direction to be along one of the principal axes of the cell, because the infinite directions of the system are easily implemented by periodic (or reflective) boundary conditions on the respective boundaries of the cell. Furthermore, let the "bottom" boundary be reflective as well, so that the model represents the half-thickness of a slab. Consider a tally plane with its normal vector along the finite direction, cutting through the entire cell. Because of symmetry, the net current through the plane can only be oriented along the finite direction, and the same holds for the gradient of the flux. Furthermore, because the all the other boundaries except the tally plane are reflective, the total leakage from the cell is only through the tally plane. The diffusion coefficient at a tally plane i may then be defined as[8]:

$$D_i = \frac{J_{\text{net,i}}}{d\phi(z)/dz|_i} \tag{1}$$

where z is considered to be the finite direction of the system. Since the tally planes cuts through the entire cell, the diffusion coefficient represents an "averaged" material at the tally plane location.

2. Neutron tallies and modeling of the flux gradient

The gradient of the flux cannot be tallied directly, and thus a model is required. We have used four models to estimate the flux gradient from the flux tallies. The homogenized version of our geometry is really a homogeneous slab, and it is known from diffusion theory that the flux obeys a cosine-shape in that case. Also in lattice theory, the global flux shape is assumed to be a cosine. **Model 1** assumes that there is one, unique diffusion coefficient for the lattice. Then, one infers that the current should obey a sine-function:

$$\begin{aligned} \phi(z) &= A_0 \cos(B_z z) \\ J(z) &= A_1 \sin(B_z z) \end{aligned} \tag{2}$$

The diffusion coefficient then reduces to just one value, i.e.

$$D = \frac{A_1}{A_0 B_z} \tag{3}$$

In this model, the buckling B_z is fitted using flux and current tallies simultaneously, while the amplitudes A_0 and A_1 are fitted individually. This estimator is very robust to the quality of the flux and current tallies (any "erratic" behavior is smoothed out in the fitting procedure). But the model makes the very strong assumption that there is a unique diffusion coefficient. Application of this model is illustrated later.

Model 2 assumes a cosine shape for the flux, to give

$$\phi(z) = A_0 \cos(B_z z) \Rightarrow \frac{d\phi(z)}{dz} = -A_0 B_z \sin(B_z z) \tag{4}$$

The parameters A_0 and B_z are derived from the flux tallies. This model is less robust than the first model. It is not very sensitive to the quality of the flux tallies, but the current tallies need to be well-behaved for use in equation (1).

Model 3 uses a cubic spline fit to the flux tally results. In this case, the derivative d_i at each tally plane is obtained directly. This model is least robust, because it is sensitive to the smoothness of the current and the flux tallies. A small error in the flux tallies may cause a rather large error in the derivative d_i, which in turn results in a poor estimation of the diffusion coefficient. From a physical point of view this model may be said to be the best, because the local flux gradient and the local current tallies are used directly, with a minimum of modeling.

Model 4 relies on the definition of the diffusion coefficient from lattice physics, where the diffusion coefficient is defined as:

$$D = \frac{\text{Total leakage from cell}}{B^2 \times \text{Total flux in cell}} \tag{5}$$

As discussed earlier, the total leakage from a (collection of) unit cell(s) can only be through the tally plane. **Model 4** can thus be implemented by taking a current tally on the tally plane, and a flux tally over all the volumes enclosed by the cell boundaries and the tally plane. The buckling can be found from a cosine fit to scalar flux tallies at the tally planes.

(a) Discussion of tally plane location

If the symmetry axis of the unit cell is along the finite direction, such as a pin cell with the finite direction along the pin, the location of the cross-cutting tally planes is never an issue. This is the typical situation analysed by Milgram for CANDU cells[8] and also by us for LMFBR cells[5]. In the case of three-dimensional plate cells the situation is more complicated. Consider the case that the plates are perpendicular to the finite axis (for example, plates oriented in the x, y plane, forming a finite stack in the z-direction). The flux will show a global cosine shape superimposed with a fine structure due to the individual plates in the cell. Thus, to properly tally the global flux shape, it is critical that each tally plane is located at the same location within a cell. To say differently: the tally planes must be offset an integer times the cell dimension. However, this is not enough. The current tallies will record the "local" currents whereas the flux shape is global. To remove this inconsistency,

the currents should be tallied on the boundary of the cell. If the lattice is infinite, the current will exactly disappear on the cell boundaries. Thus, in the finite system, the current on the boundary of the cell is solely due to the "global" finiteness of the system rather than the individual nature of the plates. Taking the tallies between the unit cells also implies that the total flux used in **model 4** is the cell-integrated flux.

3. Statistical considerations

At each tally plane, one should take tallies of the partial currents j^+ and j^-, and also the total current $j^+ + j^-$. For the net current $J_{\text{net}} = j^+ - j^-$, the standard deviation is:

$$\sigma_{x-y}^2 = \sigma_x^2 + \sigma_y^2 - 2\sigma_{xy} \tag{6}$$

where x and y represent statistical quantities. The covariance of the partial currents, σ_{xy} can be calculated from the tally of the total current $j^+ + j^-$. For this sum, one finds:

$$\sigma_{x+y}^2 = \sigma_x^2 + \sigma_y^2 + 2\sigma_{xy} \Rightarrow \sigma_{x-y}^2 = 2\sigma_x^2 + 2\sigma_y^2 - \sigma_{x+y}^2 \tag{7}$$

The standard deviation of the diffusion coefficient can be calculated using:

$$\sigma_{\frac{x}{y}}^2 = \frac{x^2}{y^2}\left(\frac{\sigma_x^2}{x^2} + \frac{\sigma_y^2}{y^2} - 2\frac{\sigma_{xy}}{xy}\right) \tag{8}$$

This last equation is somewhat problematic in that it requires knowledge of the covariance between J_{net} and $\nabla\phi$, and knowledge of the error of $\nabla\phi$, both of which are unknown. As indicated by Milgram[8] it is possible to obtain estimates of the error of the derivative of a fitted function, but a literature survey did not yield any useful results. In the present research, only the error on the current is taken into account in the calculation of the diffusion coefficient, with the caveat that the resulting error will be underestimated. If a total of I samples of the diffusion coefficient are used, the average diffusion coefficient is calculated as:

$$\bar{D} = \frac{1}{I}\sum_{i=1}^{I} D_i \tag{9}$$

The standard deviation is calculated as

$$\sigma_{\bar{D}} = \sqrt{\frac{1}{I-1}\sum_{i=1}^{I}\left(D_i - \bar{D}\right)^2} \tag{10}$$

The 95% confidence interval (CI) is calculated as:

$$\bar{D} - 1.96\frac{\sigma_{\bar{D}}}{\sqrt{I}} \leq CI \leq \bar{D} + 1.96\frac{\sigma_{\bar{D}}}{\sqrt{I}} \tag{11}$$

One faces the problem that some of the diffusion coefficients D_i can be considered to be "statistical outliers". Rather than using some ad-hoc procedure to discard these results, the following model was found to be helpful. The diffusion coefficient is calculated using equation (3). Results D_i which are more than 25% different from the diffusion coefficient calculated from equation (3) are discarded from further analysis, as are any results with an estimated error of more than 25%.

It is common in Monte Carlo calculations to reduce as much as possible the volume of the calculational domain, because better statistics will be obtained for the same number of neutron histories. However, in the case of the modelling of a three-dimensional plate cell, the overall volume of the geometrical model is determined by the dimensions of the unit cell and the number of cells used in the calculation. Improved statistics can only be obtained by increasing the number of neutron histories.

III. Calculations

1. Models

In the present study we have investigated plate cell C11 as used in the MZA series of measurements of the MOZART programme in the ZEBRA facility[9]. In ZEBRA assemblies were used with sodium plates and void plates. The MZA C11 cell is symmetric and consists of a stack of plates of various materials. Fuel and sodium plates have cladding, while bare plates of stainless steel and graphite are inserted to obtain proper material volume fractions and neutron spectrum. The analysis is done with the continuous energy Monte Carlo code MVP[10]. The dimensions of the ZEBRA cells are $5.4254 \times 5.4254 \times 7.4958$ ($\Delta x \times \Delta y \times \Delta z$) cm. In all calculations, the plates are oriented horizontally. One model named `c11_z` consists of 15 cells stacked on top of each other, reflected on all sides except the positive z-face, which is open to vacuum. The second model named `c11_x` consists of 20 cells stacked left to right, with all sides reflected except the positive x-face, which is open to vacuum. The sizes are chosen to obtain $B \approx 1.5 \times 10^{-2}$ cm^{-1} which is representative of the ZEBRA facility.

Commonly one replaces the 3D cell with a 1D equivalent cell, but this introduces some non-physical approximations. For example, a 3D void area surrounded by cladding is not the same as its 1D equivalent (a low density slab). Furthermore, in the 1D cell the background cross section for resonant isotopes is different from the actual 3D cell. Thus the question is whether or not one can use a 1D equivalent model in the calculation of the diffusion coefficient without and with voided areas. Thus 2 geometrical descriptions are used in our Monte Carlo calculations: a full 3D model, and a 1D model where each plates is represented as a homogenized mixture. A-priori homogenization is done with simple volume weighting. The cells are illustrated in **Fig.** 2. Continuous energy calculations mean that self-shielding issues do not arise. MVP settings are reported in **Table** 1. Results are tallied in 7 energy groups, and energy boundaries are given in **Table** 2.

In the conventional Benoist-formalism, the parallel diffusion coefficient, i.e. the diffusion coefficient corresponding to `c11_x`, becomes infinite if there are planar voids. Strictly speaking, this situation can only occur in the 1D model. But the 1D model has "smeared" plates, in which there are no true void regions. With these low density regions the Benoist-style parallel diffusion coefficient is not infinite, but likely to be erroneous. In practice, the perpendicular and parallel diffusion

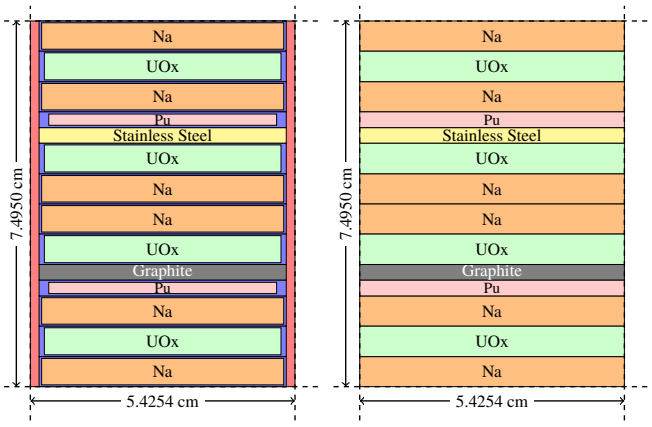

Fig. 2 Models of the ZEBRA C11 unit cell. Left: full 3D model, right: simplified 1D model in which the materials of each plate are homogenized.

Table 1 Settings used for MVP calculations.

MVP parameter	Value
`NHIST`	36.000
`KBATCH`	20.000
`NSKIP`	200

Table 2 Energy boundaries used in the MVP tallies.

Group	Upper energy boundary [eV]
1	1.00000×10^{7}
2	3.67879×10^{6}
3	1.35335×10^{6}
4	86.5270×10^{3}
5	4.30743×10^{3}
6	2.03468×10^{3}
7	214.454×10^{0}
	1.00000×10^{-5}

coefficients are often used to quantify directional streaming effects. Under void situations the question then arises whether the "directionality" is due to physical effects or the divergence of the parallel diffusion coefficient. In our work on hexagonal LMFBR pin cells [5)] it was found that the directional dependence of the diffusion coefficient disappeared when the analysis was performed with MOC or Monte Carlo.

2. Results

The figures and tables require a lot of space. To not interrupt the text too much, figures and tables corresponding to this section have been moved to the end of this paper. Only a few results are illustrated here in graphs. A full set of results is available from the authors.

We start the discussion of the results by comparison of the 3D z and x models with sodium present. Illustrated are the diffusion coefficients obtained at each tally plane, using the cosine-fit model (**Fig.** 3 for z and **Fig.** 6 for x), the cubic spline fit (**Fig.** 4 for z and **Fig.** 7 for x), and the model of equation (5) in **Fig.** 5 for z and **Fig.** 8 for x. A rather surprising find is the very strong trends of the diffusion coefficient in the z-model. Trends are not so strong in the x-model. The trends in the z-model are much stronger than the errors associated with the individual diffusion coefficients, and are present in all z-direction calculations, regardless of geometrical detail or the presence of sodium. As a result of the trends the confidence intervals become large, which means that discussions about whether sets of results are statistically different or not becomes difficult.

The four different models to calculate the diffusion coefficient all result in similar results, as illustrated in **Table** 3 and **Table** 4, providing confirmation that the Monte Carlo method is valid. It is noted that **model 4** leads to a systematicly lower estimate of the diffusion coefficient. The confidence intervals of the diffusion coefficient become very large in some cases. This is due to trending (z-model) and in the low-energy groups due to a low number of tally scores. Both these effects indicate the limitations of the Monte Carlo analysis methods. In Tables 3 and 4 one can compare the diffusion coefficients between the 3D cell and the simple 1D cell. In all cases, the simple 1D model yields diffusion coefficients which are slightly smaller than the 3D model. It seems reasonable to do the analysis with the simple 1D model, and if desired one can define bias factors for the diffusion coefficients. This confirms the physical expectation that the 1D model should be adequate. The decrease of the diffusion coefficient between the 3D and 1D models is physically reasonable. In the 3D model, a neutron traveling in a void will only undergo attenuation between the voids, whereas in the 1D model the neutron will always undergo attenuation. It is expected that the distance the neutron travels while diffusing through the media will thus be smaller in the 1D model.

The effect of directionality is similar between the 3D and the 1D cells. Diffusion coefficients show a directional dependence, especially in the lower energy groups, as illustrated in **Table** 5. This confirms the expectation that neutron diffusion parallel to the plates is different from neutron diffusion perpendicular to the plates. However, if the Benoist-formalism is used, the directional dependence can be overestimated for void conditions due to the divergence of the parallel diffusion coefficient.

3. Discussion

In the course of the presented work a discussion arose about what could be considered to be the "exact" value of the diffusion coefficient, and whether or not the Monte Carlo method is capable of calculating a "benchmark value" of the diffusion coefficient. With "benchmark value" we mean some calculated value which in the limit of an infinite number of neutron histories converges to the "real" value. Unfortunately, this is impossible for the diffusion coefficient because the Monte Carlo method cannot directly tally the diffusion coefficient. In fact, one cannot tally the derivative of the flux. Thus, one always needs some sort of model to obtain the diffusion coefficient from the tally results. The resulting value cannot be considered a benchmark value, because if the model is wrong, then in the limit of an infinite number of histories, the result will still

have a systematic error due to modeling error. Thus, one must be satisfied with "best estimate" values of the diffusion coefficient within a certain theoretical framework, rather than "exact values".

IV. Conclusions

A model to calculate the diffusion coefficient for 3D plate cells with Monte Carlo techniques was successfully developed. The presented method relies solely on standard Monte Carlo techniques, and no modifications were needed in the MVP code. The model is unique in that it allows to calculate the diffusion coefficient of complicated unit cells, and it allows to check whether modeling assumptions are valid, and could be used to define bias factors to be used in simplified analyses.

The strong trends seen in the z-model are surprising. The trends are independent of modeling detail, flux gradient estimation and presence of voids. It seems then that it is a physical effect rather than an artifact of the calculation, and the diffusion coefficients of the various cells are physically different. The cause of the trends has not been identified and will be investigated in the future with deterministic multi-group methods. One expects an influence of the neutron spectrum in the different unit cells. The issue of the neutron spectrum is fundamental to lattice theory, where one analyses a "deep interior" cell far removed from any physical boundaries of the system.

It is found that the replacement of the full 3D model with the simplest 1D model results in a slight reduction of the diffusion coefficient (in the order of 1%), whether sodium is present or not. Directional dependence is different between the 3D and 1D models, but a trend cannot be identified. It thus seems that the classic analysis based on a simplified 1D cell description is justified, where our new method can provide bias factors if desired.

A final note on calculation time: since the volume of the model in the Monte Carlo analysis cannot be made arbitrarily small in the present work, the only way to improve statistics is to run more neutron histories. This also applies to the low energy region, which is always troublesome in the Monte Carlo analysis of fast neutron systems. At present, computation times are such that routine analysis on workstations is not feasible.

In the future our new method will be used for pin-type cell calculations of LMFBRs, for instance to estimate the influence on the diffusion coefficient of the explicit modeling of the wrapper tube, and to analyse the problem of fuel assemblies with a so-called inner duct, which represents a strong streaming path under both sodium flooded and sodium void conditions.

References

1) Valentine C. Deniz. *The CRC Handbook of nuclear reactor calculations*, volume II, chapter The theory of neutron leakage in reactor lattices, 409 - 504. CRC Press, Boca Raton, FL, USA (1986).

2) G. Rimpault. *Physics documentation of ERANOS: The ECCO cell code*. CEA, Centre d'Etudes de Cadarache, France (October 1997). Rapport Technique H0 - 5010 - 430 - 5420.

3) Taira Hazama, Go Chiba, Wakaei Sato, and Kazuyuki Numata. *SLAROM-UF: Ultra-Fine Group Cell Code for Fast Reactor*. JAEA (May 2009). JAEA-Review 2009-023.

4) Ely M. Gelbard. *Advances in Nuclear Science and Technology*, volume 15, chapter Streaming in Lattices, 223 - 400. Plenum Press (1983).

5) W.F.G. van Rooijen and G. Chiba. "Diffusion coefficients for LMFBR cells calculated with MOC and Monte Carlo methods." *Annals of Nuclear Energy* (2010). Accepted for publication.

6) Ely M. Gelbard and Richard Lell. "Monte Carlo treatment of fundamental-mode neutron leakage in the presence of voids." *Nuclear Science and Engineering*, **63**:9 - 23 (1977).

7) S.S. Gorodkov and M.A. Kalugin. "Monte Carlo calculation of the diffusion coefficient of nuclear reactor cells." *Atomic Energy*, **106**(4):231 - 237 (2009). doi: 10.1007/s10512-009-9157-7.

8) M.S. Milgram. "Estimation of axial diffusion processes by analog Monte-Carlo: theory, tests and examples." *Annals of Nuclear Energy*, **24**(9):671 - 704 (1997). PII: S0306-4549(96)00049-7.

9) John Rowlands, Atsushi Zukeran, Masayuki Nakagawa, Peter Smith, and Udo K. Wehmann. "The ZEBRA MOZART programme. part 1. MZA and MZB Zebra assemblies 11 and 12." (January 2008). URL `http://www.zebra.webnik.org`.

10) Yasunobu Nagaya, Keisuke Okumura, Takamasa Mori, and Masayuki Nakagawa. *MVP/GMVP II: General Purpose Monte Carlo Codes for Neutron and Photon Transport Calculations based on Continuous Energy and Multigroup Methods*. JAERI (June 2005). Report JAERI-1348.

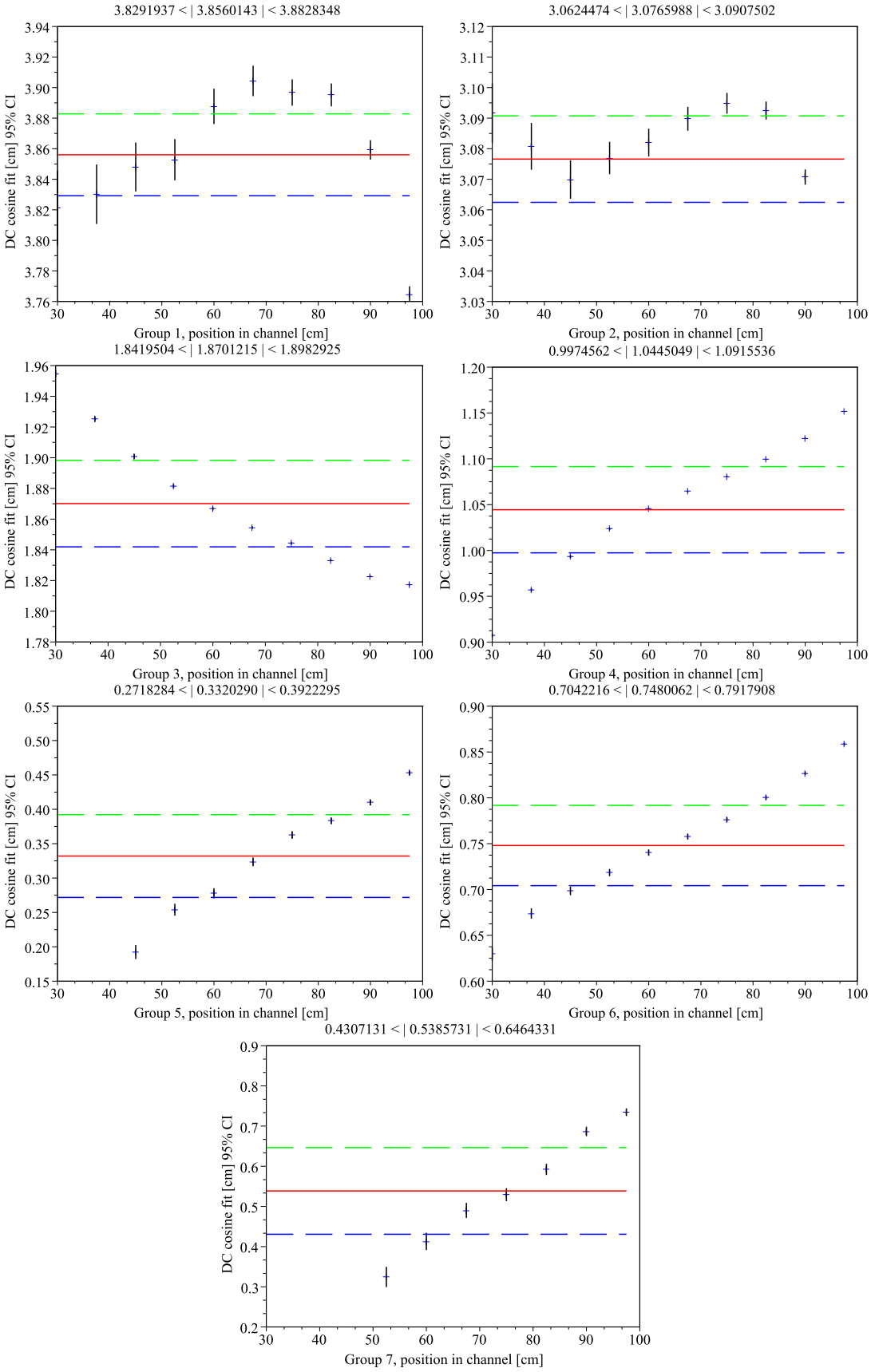

Fig. 3 Model `c11_z`, diffusion coefficients estimated using the cosine model for the flux gradient.

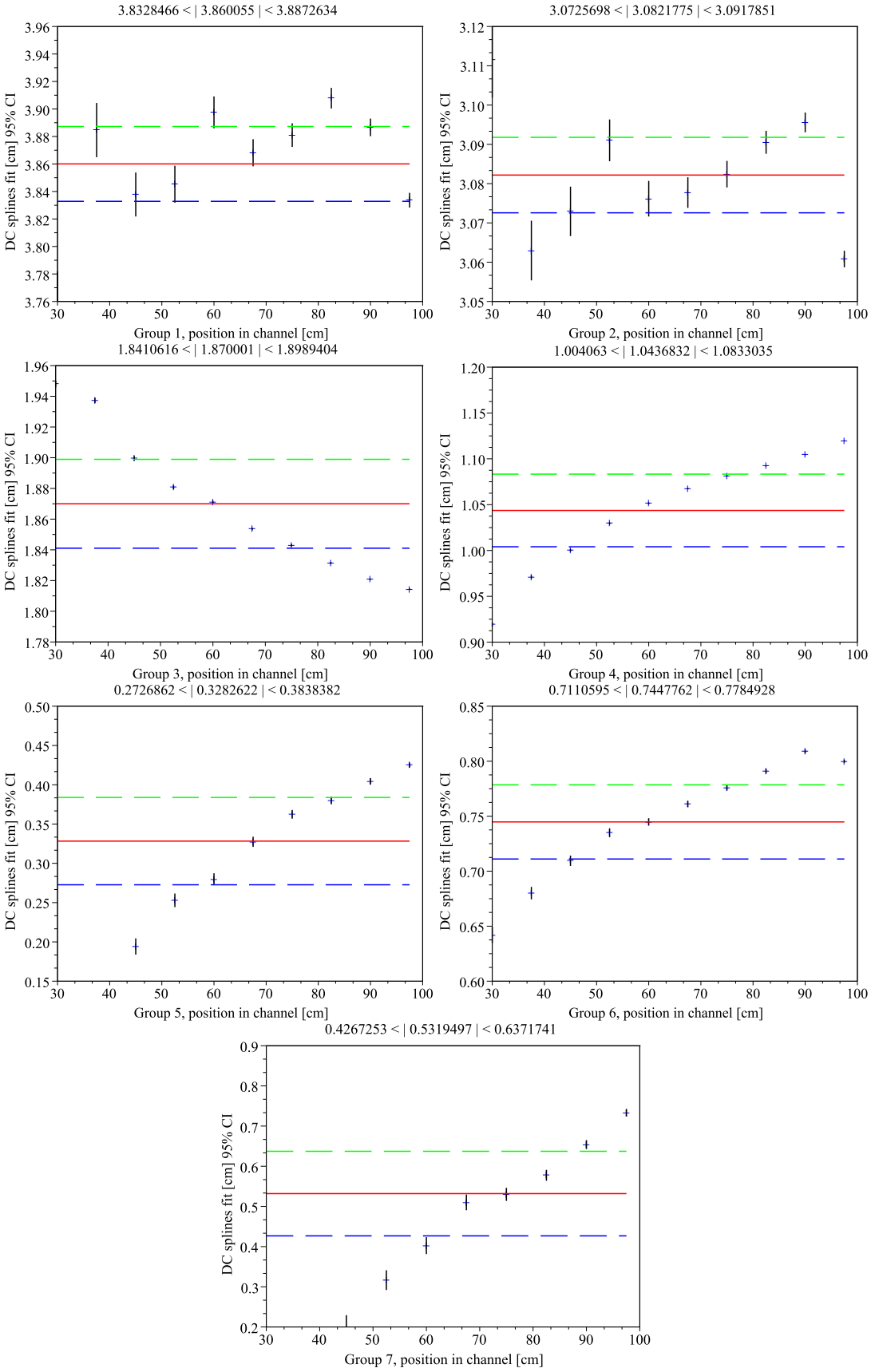

Fig. 4 Model `c11_z`, diffusion coefficients estimated using the cubic spline model for the flux gradient.

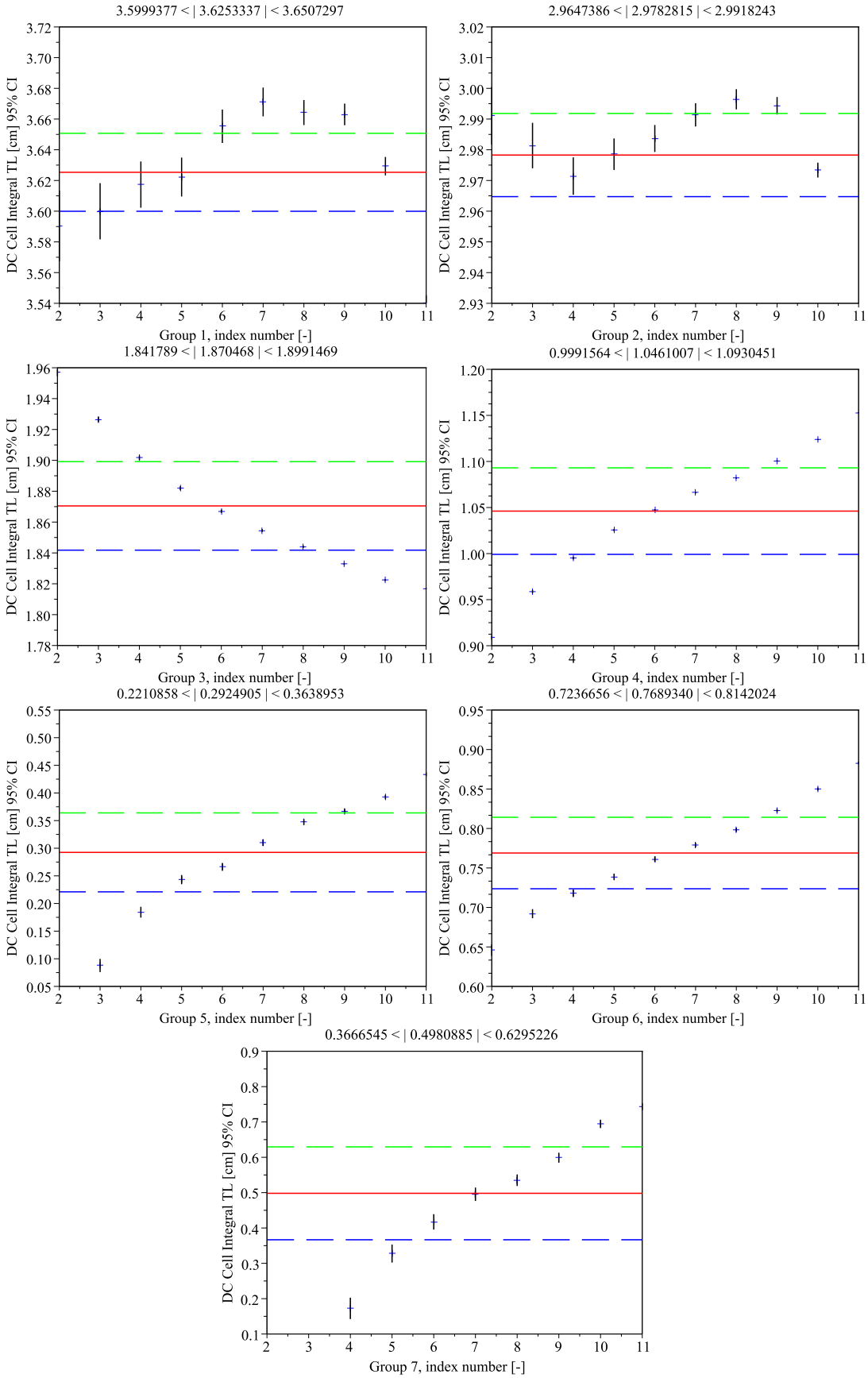

Fig. 5 Model `c11_z`, diffusion coefficients estimated using **model 4** (ratio of leakage rate to integrated flux).

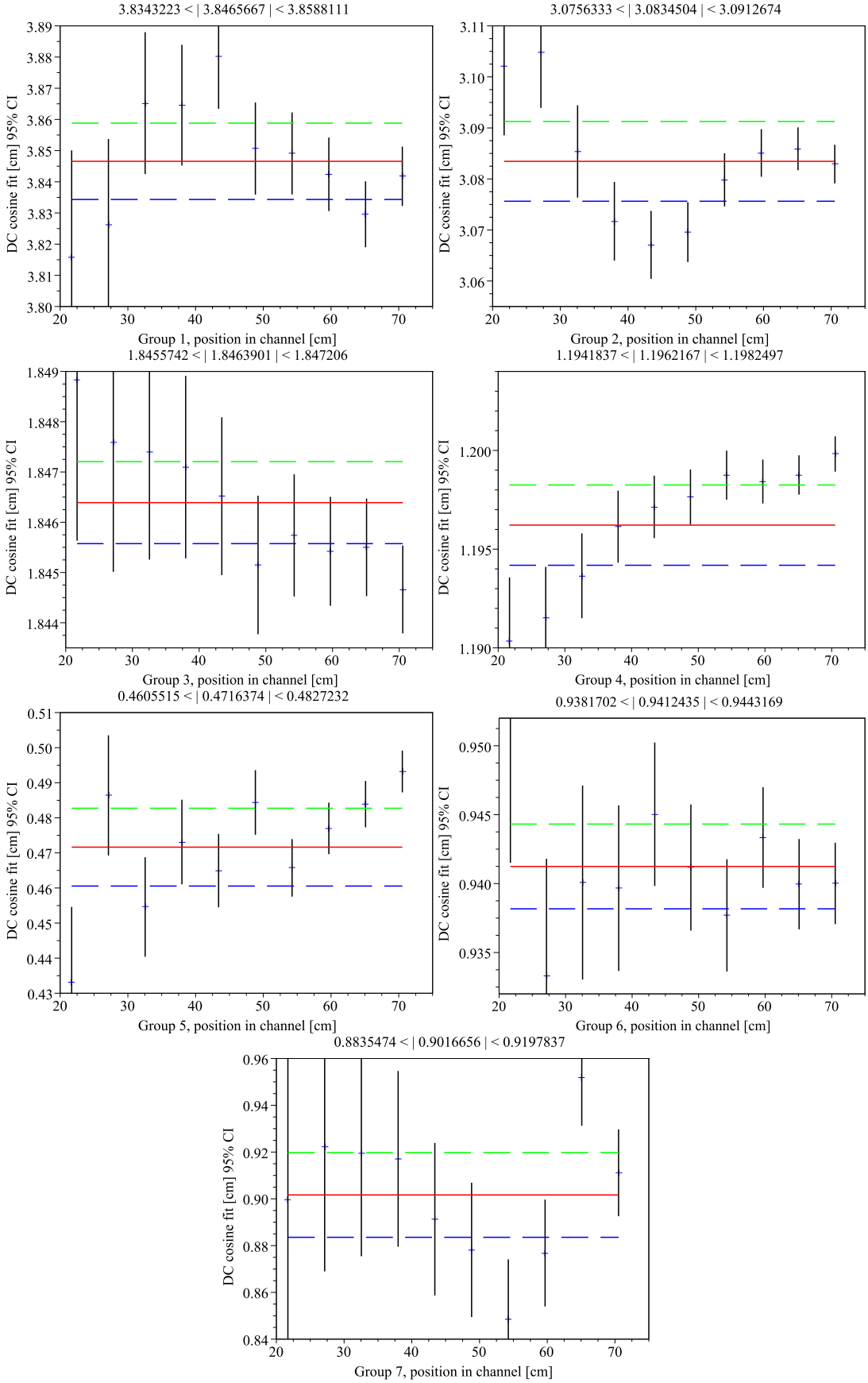

Fig. 6 Model `c11_x`, diffusion coefficients estimated using the cosine model for the flux gradient.

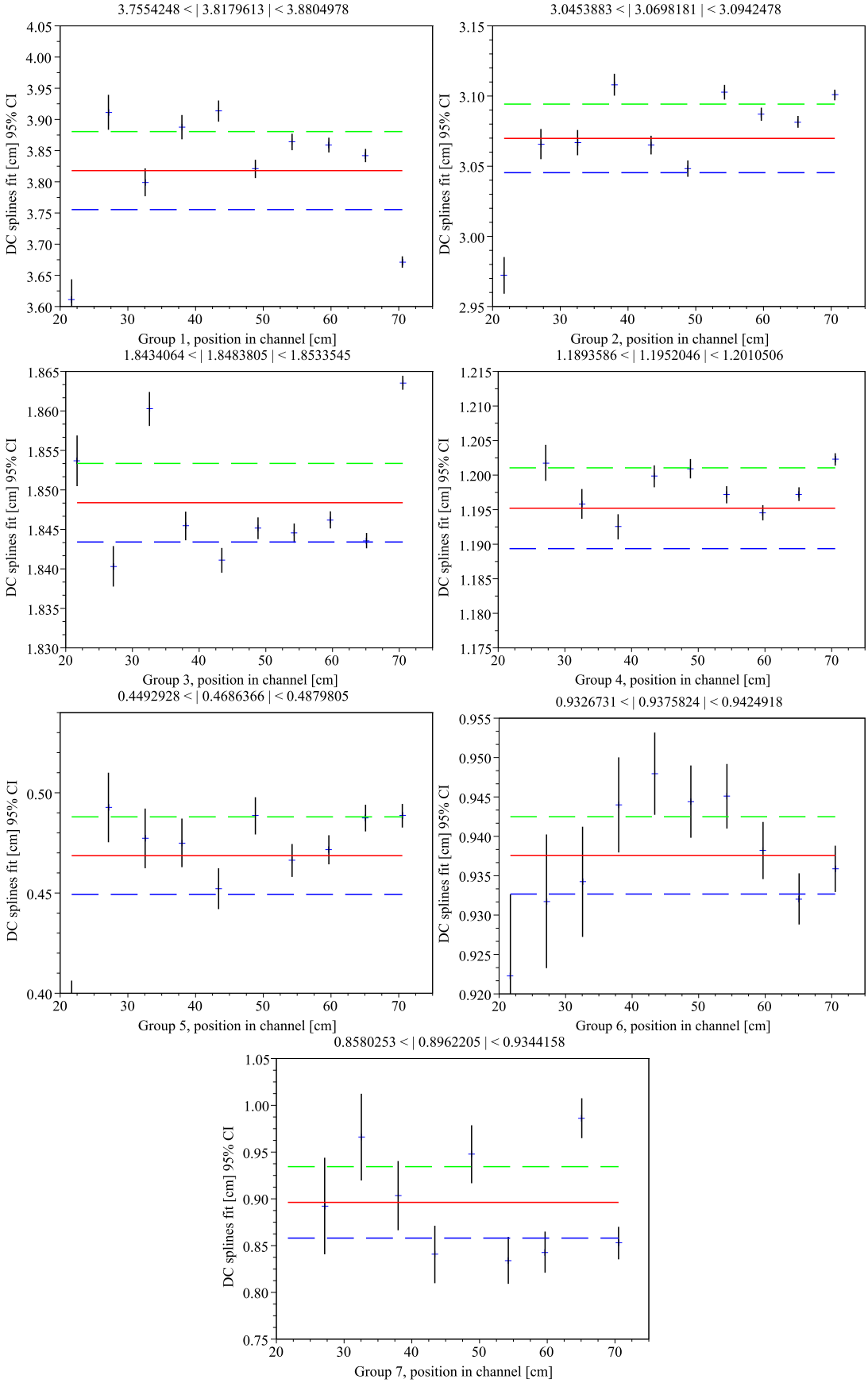

Fig. 7 Model `c11_x`, diffusion coefficients estimated using the cubic spline model for the flux gradient.

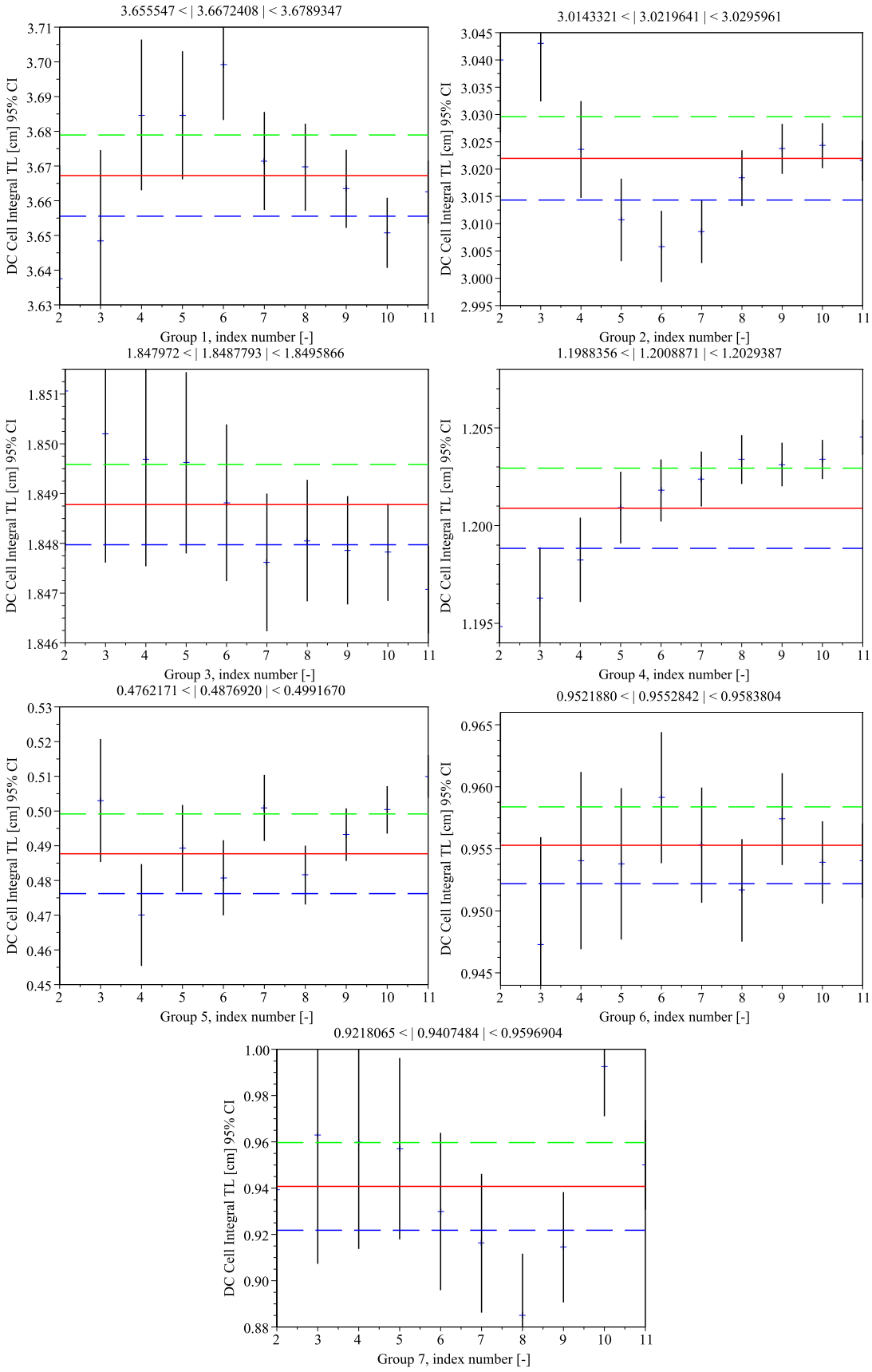

Fig. 8 Model `c11_x`, diffusion coefficients estimated using **model 4** (ratio of leakage rate to integrated flux).

Table 3 Diffusion coefficients for `c11_z`. D_s: **model 1**; $D_{\cos}$: **model 2**; D_{spline}: **model 3**; D_{TL}: **model 4**.

gr	D_s	$D_{\cos}$	D_{spline}	D_{TL}	CI cos	CI spline	CI TL
`c11_z`, 3D model, Sodium present							
1	3.858	3.856	3.860	3.625	3.829 ↔ 3.883	3.833 ↔ 3.887	3.600 ↔ 3.651
2	3.073	3.077	3.082	2.978	3.062 ↔ 3.091	3.073 ↔ 3.092	2.965 ↔ 2.992
3	1.851	1.870	1.870	1.870	1.842 ↔ 1.898	1.841 ↔ 1.899	1.842 ↔ 1.899
4	1.077	1.045	1.044	1.046	0.997 ↔ 1.092	1.004 ↔ 1.083	0.999 ↔ 1.093
5	0.335	0.332	0.328	0.292	0.272 ↔ 0.392	0.273 ↔ 0.384	0.221 ↔ 0.364
6	0.779	0.748	0.745	0.769	0.704 ↔ 0.792	0.711 ↔ 0.778	0.724 ↔ 0.814
7	0.507	0.539	0.532	0.498	0.431 ↔ 0.646	0.427 ↔ 0.637	0.367 ↔ 0.630
`c11_z`, 1D model, Sodium present							
1	3.835	3.826	3.851	3.593	3.793 ↔ 3.860	3.796 ↔ 3.906	3.561 ↔ 3.625
2	3.065	3.068	3.066	2.968	3.054 ↔ 3.081	3.049 ↔ 3.083	2.955 ↔ 2.981
3	1.836	1.856	1.862	1.856	1.827 ↔ 1.884	1.822 ↔ 1.901	1.827 ↔ 1.885
4	1.069	1.036	1.037	1.038	0.989 ↔ 1.083	1.000 ↔ 1.074	0.991 ↔ 1.085
5	0.326	0.319	0.315	0.281	0.253 ↔ 0.384	0.255 ↔ 0.376	0.207 ↔ 0.354
6	0.768	0.737	0.734	0.762	0.692 ↔ 0.782	0.697 ↔ 0.771	0.715 ↔ 0.809
7	0.472	0.504	0.498	0.468	0.393 ↔ 0.614	0.401 ↔ 0.596	0.338 ↔ 0.598
`c11_z`, 3D model, Sodium void							
1	4.339	4.345	4.332	4.159	4.310 ↔ 4.381	4.253 ↔ 4.411	4.125 ↔ 4.193
2	3.554	3.563	3.561	3.479	3.543 ↔ 3.583	3.544 ↔ 3.578	3.460 ↔ 3.499
3	2.228	2.245	2.246	2.250	2.220 ↔ 2.269	2.215 ↔ 2.277	2.225 ↔ 2.275
4	1.269	1.230	1.229	1.230	1.174 ↔ 1.285	1.187 ↔ 1.271	1.175 ↔ 1.285
5	0.803	0.760	0.753	0.760	0.699 ↔ 0.821	0.695 ↔ 0.811	0.699 ↔ 0.821
6	0.879	0.820	0.816	0.817	0.735 ↔ 0.905	0.738 ↔ 0.894	0.732 ↔ 0.903
7	0.552	0.581	0.564	0.532	0.448 ↔ 0.714	0.455 ↔ 0.672	0.386 ↔ 0.677
`c11_z`, 1D model, Sodium void							
1	4.314	4.318	4.301	4.128	4.286 ↔ 4.351	4.234 ↔ 4.368	4.096 ↔ 4.159
2	3.545	3.553	3.558	3.465	3.532 ↔ 3.574	3.549 ↔ 3.568	3.445 ↔ 3.485
3	2.212	2.229	2.231	2.234	2.204 ↔ 2.255	2.198 ↔ 2.263	2.208 ↔ 2.260
4	1.256	1.217	1.215	1.218	1.163 ↔ 1.272	1.171 ↔ 1.259	1.164 ↔ 1.273
5	0.789	0.748	0.743	0.748	0.689 ↔ 0.806	0.692 ↔ 0.794	0.689 ↔ 0.807
6	0.864	0.804	0.798	0.803	0.717 ↔ 0.890	0.717 ↔ 0.880	0.716 ↔ 0.890
7	0.508	0.541	0.539	0.539	0.431 ↔ 0.650	0.439 ↔ 0.639	0.430 ↔ 0.648

Table 4 Diffusion coefficients for `c11_x`. D_s: **model 1**; $D_{\cos}$: **model 2**; D_{spline}: **model 3**; D_{TL}: **model 4**.

gr	D_s	$D_{\cos}$	D_{spline}	D_{TL}	CI cosine	CI spline	CI TL
`c11_x`, 3D model, Sodium present							
1	3.847	3.847	3.818	3.667	3.834 ↔ 3.859	3.755 ↔ 3.880	3.656 ↔ 3.679
2	3.081	3.083	3.070	3.022	3.076 ↔ 3.091	3.045 ↔ 3.094	3.014 ↔ 3.030
3	1.846	1.846	1.848	1.849	1.846 ↔ 1.847	1.843 ↔ 1.853	1.848 ↔ 1.850
4	1.198	1.196	1.195	1.201	1.194 ↔ 1.198	1.189 ↔ 1.201	1.199 ↔ 1.203
5	0.477	0.472	0.469	0.488	0.461 ↔ 0.483	0.449 ↔ 0.488	0.476 ↔ 0.499
6	0.941	0.941	0.938	0.955	0.938 ↔ 0.944	0.933 ↔ 0.942	0.952 ↔ 0.958
7	0.901	0.902	0.896	0.941	0.884 ↔ 0.920	0.858 ↔ 0.934	0.922 ↔ 0.960
`c11_x`, 1D model, Sodium present							
1	3.645	3.650	3.691	3.650	3.639 ↔ 3.660	3.580 ↔ 3.802	3.640 ↔ 3.660
2	3.005	3.002	3.010	3.002	2.996 ↔ 3.007	2.982 ↔ 3.039	2.996 ↔ 3.007
3	1.828	1.828	1.828	1.828	1.827 ↔ 1.829	1.824 ↔ 1.832	1.827 ↔ 1.829
4	1.184	1.183	1.184	1.183	1.182 ↔ 1.184	1.178 ↔ 1.189	1.183 ↔ 1.184
5	0.487	0.485	0.483	0.485	0.477 ↔ 0.494	0.475 ↔ 0.490	0.477 ↔ 0.494
6	0.928	0.925	0.924	0.925	0.919 ↔ 0.932	0.903 ↔ 0.944	0.918 ↔ 0.932
7	0.921	0.905	0.936	0.904	0.881 ↔ 0.929	0.837 ↔ 1.034	0.881 ↔ 0.928
`c11_x`, 3D model, Sodium void							
1	4.469	4.471	4.477	4.276	4.463 ↔ 4.480	4.447 ↔ 4.507	4.268 ↔ 4.283
2	3.681	3.683	3.669	3.615	3.679 ↔ 3.686	3.635 ↔ 3.703	3.611 ↔ 3.618
3	2.367	2.368	2.369	2.370	2.367 ↔ 2.368	2.356 ↔ 2.382	2.369 ↔ 2.371
4	1.500	1.499	1.502	1.504	1.497 ↔ 1.501	1.494 ↔ 1.510	1.502 ↔ 1.506
5	1.002	0.998	0.991	1.015	0.993 ↔ 1.004	0.970 ↔ 1.013	1.009 ↔ 1.020
6	1.145	1.142	1.136	1.168	1.138 ↔ 1.147	1.104 ↔ 1.169	1.164 ↔ 1.172
7	1.046	1.041	1.050	1.086	0.991 ↔ 1.092	0.995 ↔ 1.104	1.033 ↔ 1.138
`c11_x`, 1D model, Sodium void							
1	4.243	4.246	4.271	4.245	4.238 ↔ 4.253	4.189 ↔ 4.353	4.238 ↔ 4.253
2	3.577	3.575	3.583	3.575	3.571 ↔ 3.580	3.559 ↔ 3.606	3.571 ↔ 3.579
3	2.316	2.318	2.317	2.317	2.315 ↔ 2.320	2.313 ↔ 2.321	2.315 ↔ 2.319
4	1.452	1.450	1.452	1.450	1.447 ↔ 1.453	1.446 ↔ 1.457	1.448 ↔ 1.453
5	0.971	0.972	0.960	0.972	0.965 ↔ 0.978	0.934 ↔ 0.986	0.965 ↔ 0.978
6	1.122	1.120	1.124	1.120	1.115 ↔ 1.126	1.108 ↔ 1.141	1.115 ↔ 1.126
7	0.992	1.002	0.974	1.006	0.976 ↔ 1.027	0.910 ↔ 1.037	0.980 ↔ 1.032

Table 5 Directional dependence of the diffusion coefficients. Diffusion coefficients based on **model 4** are used. Directional dependence is strong in the low energy groups. Note the unexpected result in group 5, where the directional dependence is smaller in the voided situation. This is probably due to the change of the neutron spectrum upon voiding.

Group	D_z	D_x	$\frac{D_x - D_z}{D_z}$ [%]	D_z	D_x	$\frac{D_x - D_z}{D_z}$ [%]
	3D model, sodium present			3D model, sodium absent		
1	3.625	3.667	1.159	4.159	4.276	2.813
2	2.978	3.022	1.148	3.479	3.615	3.909
3	1.870	1.849	-1.123	2.250	2.370	5.333
4	1.046	1.201	14.82	1.230	1.504	22.28
5	0.292	0.488	67.23	0.760	1.015	33.55
6	0.769	0.955	24.19	0.817	1.168	42.96
7	0.498	0.941	88.96	0.532	1.086	104.1
	1D model, sodium present			1D model, sodium absent		
1	3.593	3.650	1.586	4.128	4.245	2.834
2	2.968	3.002	1.146	3.465	3.575	3.175
3	1.856	1.828	-1.509	2.234	2.317	3.715
4	1.038	1.183	13.97	1.218	1.450	19.05
5	0.281	0.485	72.60	0.748	0.972	29.95
6	0.762	0.925	21.39	0.803	1.120	39.48
7	0.468	0.904	93.16	0.539	1.006	86.64